Simulations of Polymer Cyclization by Brownian Dynamics

Alexei Podtelezhnikov and Alexander Vologodskii*

Department of Chemistry, New York University, 29 Washington Place, New York, New York 10003

Received March 20, 1997; Revised Manuscript Received July 28, 1997[⊗]

ABSTRACT: The dynamic characteristics of polymers in dilute solution, such as the end-to-end distance relaxation time, τ_m, and the time of diffusion-controlled cyclization, τ_a, were studied using Brownian dynamics simulations. The major goal was to estimate the effect of the impenetrability of the chain backbone on the dynamic properties. We compared several models of polymer chains: phantom ones with and without excluded volume and a nonphantom model with excluded volume. The hydrodynamic interaction between chain segments was not taken into account. The impenetrability of a chain is found to have a small effect on the magnitude of τ_m. For sufficiently long chains, τ_m exceeded the value for phantom chains by factor of 1.5. The ratio τ_a/τ_m remained the same for the phantom and nonphantom models. On the other hand, the excluded volume effect changed the dependence of τ_m on the chain contour length, in accordance with the known theoretical conclusions. In addition, the presence of excluded volume caused a 2-fold increase of the scaling factor between τ_a and τ_m for sufficiently long chains. This scaling factor and, consequently, τ_a appeared to be reciprocally proportional to the reaction radius R. When the reaction radius is close to the statistical segment length l, τ_a was estimated as $\tau_a = \zeta(l/R)\tau_m$, where the coefficient ζ is equal to 1.3 ± 0.2 and 2.6 ± 0.3 for chains without and with excluded volume, respectively.

I. Introduction

Since the pioneering studies of polymer dynamics by Rouse[1] and Zimm,[2] considerable theoretical progress has been achieved in this field. This includes the treatment of a more realistic polymer model, the wormlike chain,[3] and the inclusion of excluded volume effects.[4] In the early 70s Wilemski and Fixman analyzed diffusion-controlled kinetics of polymer cyclization.[5−7] This subject received further development in subsequent years.[8−13] In general, the theoretical results are in a good qualitative agreement with the experimental data, although there are important quantitative discrepancies (see the review in ref 14). It is often difficult to vary parameters of a polymer system in experimental study, and thus, a relatively limited amount of experimental data is available for comparison. Computer simulation of polymer dynamics can partly alleviate this lack of experimental data. It allows us to test the importance of different theoretical assumptions and approximations and to clarify what features of a polymer model are essential for dynamic properties. This approach is employed in the present work.

Our primary goal was to estimate the influence of chain impenetrability on the kinetics of chain cyclization in the diffusion-controlled limit. We used a Brownian dynamics (BD) algorithm[15,16] to investigate this for different models. Relatively simple but sufficiently long model chains were used in the work to study the dependence of the cyclization time on the chain length and reaction radius. We also studied the relaxation of the end-to-end distance of the model chains.

Previously, Brownian dynamics (BD) has been applied to the problem of cyclization kinetics in the diffusion-controlled limit.[17−19] Rather long chains were treated in recent studies[18,19] where the authors took into account, in some approximations, the hydrodynamic interaction between chain segments. These works gave a comprehensive picture of the cyclization kinetics, although the effect of the chain impenetrability was not studied there.

We used a straightforward approach to define the cyclization rate, based on direct observation of chain closing. This approach is expensive computationally, and to perform the analysis for relatively long chains, we did not take into account the hydrodynamic interaction between model subunits. We believe, however, that the hydrodynamic interaction should not seriously alter our estimates of the impenetrability effect on the dynamic properties of model chains.

Four models of a polymer chain were used in the study: a freely jointed model with and without excluded volume and a model with restricted flexibility (hindered random walk model) with and without excluded volume. All the chains in our simulations consisted of spherical beads as the BD algorithm requires. Impenetrability was included in the models along with excluded volume effects through sufficiently strong repulsion between the chain beads that prevented any backbone passage through itself. A weaker repulsion between beads allowed almost free backbone passage while providing a comparable value of the excluded volume effect. The effect of impenetrability on the cyclization and the end-to-end distance relaxation times was evaluated by comparison of the simulation results for the models.

II. Models and Methods of Calculations

A. Polymer Models. A polymer chain was modeled as a chain of N spherical beads so that its conformation was given by the set of coordinates of bead centers, $\mathbf{r}_i$, $i = 1, ..., N$. The total energy of the model polymer chains, E, was computed as a sum of stretching energy, E_s, energy of repulsion between colliding beads, E_p or E_r, and bending energy, E_b. We used four polymer models with different interactions involved:

$E = E_s + E_p$ (ideal freely jointed chain)

$E = E_s + E_r$ (freely jointed with excluded volume)

$E = E_s + E_p + E_b$ (ideal hindered random walk chain)

$E = E_s + E_r + E_b$ (hindered random walk with excluded volume)

[⊗] Abstract published in *Advance ACS Abstracts,* October 1, 1997.

S0024-9297(97)00391-4 CCC: $14.00

The following equations specify these energy terms.

1. Stretching. This potential kept the beads connected into the chain and thus was included in all models. We used a simple harmonic approximation for the potential

$$E_s = \frac{1}{2}\frac{kT}{\delta_s^2}\sum_{i=1}^{N-1}(b_i - b)^2 \quad (1)$$

where b_i is the length of the bond between two adjacent beads, $b_i = |\mathbf{r}_{i+1} - \mathbf{r}_i|$, b is the bond length in the relaxed state, and δ_s is a parameter of stretching rigidity. The value of δ_s is very close to the amplitude of thermal fluctuations of the bond length.

2. Bending. This kind of interaction was involved only in the hindered random walk models. The bending potential between adjacent bonds was determined by the angle between them and given by the usual harmonic expression

$$E_b = \frac{1}{2}\frac{kT}{\delta_b^2}\sum_{i=1}^{N-2}\left(\arccos\frac{\mathbf{b}_i\cdot\mathbf{b}_{i+1}}{b_i b_{i+1}}\right)^2 \quad (2)$$

where $\mathbf{b}_i$ and $\mathbf{b}_{i+1}$ are two adjacent bond vectors and δ_b is a parameter of bending rigidity of the order of mean angle between the bonds.

3. Repulsion. The excluded volume potential was defined as

$$E_r = \frac{1}{2}\frac{kT}{\delta_r^2}\sum_{i=1}^{N-2}\sum_{j=i+2}^{N}(r_{ij} - d)^2\Phi(r_{ij} - d),$$

$$\Phi(x) = \begin{cases}1, & x < 0\\ 0, & x \geq 0\end{cases} \quad (3)$$

where r_{ij} is the separation between two nonadjacent beads of diameter d, $r_{ij} = |\mathbf{r}_j - \mathbf{r}_i|$, and δ_r is a rigidity parameter. Thus, two colliding beads repelled each other according to Hooke's law when the distance between their centers was less than d.

The repulsion between beads i and $i + 2$ eliminates near-antiparallel orientations of bonds $\mathbf{b}_i$ and $\mathbf{b}_{i+1}$. This repulsion changed the length of a statistical segment, l, which was larger than that of ideal models. To compensate for that change we also included this kind of repulsion for chains without excluded volume through the potential E_p given by

$$E_p = \frac{1}{2}\frac{kT}{\delta_r^2}\sum_{i=1}^{N-2}(r_{i,i+2} - d)^2\Phi(r_{i,i+2} - d) \quad (4)$$

We will still call such chains "freely jointed" ones since most of the mutual rotations of adjacent bonds were totally free.

B. Metropolis Monte Carlo Procedure. BD simulations were started from a set of equilibrium conformations of linear chains generated by the metropolis Monte Carlo procedure.[20] Two kinds of motions were used in the procedure to construct trial conformations. The first was a randomly directed displacement of a bead within a distance range of [0, r]. The second was a swing of a single bond through some angle so that the orientation of all the other bonds remained intact. The direction of the new bond vector was randomly chosen so that the angle between the new and current directions was less than some angle ϕ. The standard rule of acceptance of a trial conformation was used.[20] The maximum amplitudes of the movements, r and ϕ, were chosen so that about half of all trial conformations were accepted.

Up to 30 000 steps were used to generate each initial conformation for BD simulation. If at the end of the Monte Carlo run a chain had its ends within the reaction radius, it was rejected, and we repeated the procedure. We also used this procedure to calculate appropriate ensemble averages of our chains such as the mean square end-to-end distance.

C. Brownian Dynamics Procedure. Our procedure was based on a second order BD algorithm[16] which was applied to a chain without hydrodynamic interaction between subunits. A trajectory of a chain was generated using the iterative equation

$$\mathbf{r}_i(t + \Delta t) = \mathbf{r}_i(t) + \frac{D_0}{kT}\mathbf{F}_i(\mathbf{r})\Delta t + \mathbf{R}_i(\Delta t)$$
$$\langle\mathbf{R}_i(\Delta t)\rangle = 0,\ \langle\mathbf{R}_i^2(\Delta t)\rangle = 6D_0\Delta t \quad (5)$$

where $\mathbf{r}_i(t)$ is the position of the bead i at time t, Δt is a time step, $\mathbf{R}_i(\Delta t)$ is a Langevin random displacement, D_0 is the diffusion coefficient of a free single bead, and $\mathbf{F}_i(\mathbf{r})$ is the net force exerted on the bead during the time step Δt. According to the first order BD algorithm proposed by Ermak and McCammon, $\mathbf{F}_i(\mathbf{r})$ is estimated as the force at the beginning of the interval Δt, $\mathbf{F}_i(\mathbf{r}) = \mathbf{F}_i(\mathbf{r}(t))$.[15] In the second-order algorithm $\mathbf{F}_i(\mathbf{r})$ is the average of the values at the beginning and at the end of the step, $\mathbf{F}_i(\mathbf{r}(t))$ and $\mathbf{F}_i(\tilde{\mathbf{r}}(t + \Delta t))$, where the position $\tilde{\mathbf{r}}(t + \Delta t)$ is tentatively generated using the first-order algorithm. The explicit equations for the forces can be obtained from the expressions for the potentials listed above, as $\mathbf{F}_i = -dE/d\mathbf{r}_i$.[21]

The end-to-end distance relaxation time, τ_m, was determined by approximating the autocorrelation function of the end-to-end distance, $\langle\mathbf{L}(0)\mathbf{L}(t)\rangle$, using a single exponential in the range from $0.67\tau_m$ to $4\tau_m$. The length of the trajectory, along which we collected the data for the autocorrelation function, was no shorter than $2000\tau_m$.

To compute the cyclization time, we counted the number of steps during a BD simulation before the chain ends (the centers of the terminal beads) came to within the distance of the reaction radius. Usually about 400 such cyclizations were observed for a particular chain length, reaction radius, and model. The values of the cyclization time were then averaged.

D. Model Parameters and Choice of the Time Step. 1. Rigidity Constants. By including the repulsion between nonadjacent beads we meant not only to take into account excluded volume effects but also to prevent chain bonds from passing through each other. This can be achieved by an appropriate choice of sufficiently small values of the stretching and repulsion rigidity constants, δ_s and δ_r, with the bead diameter being close to the bond length. To find the values of the rigidity constants that provide impenetrability of the model chains we tested the conservation of topology along the BD trajectory for a circular chain. We started the simulations from the knotted conformation (knot type 3_1) of the freely jointed chain of 20 segments, which has a very low equilibrium probability of knotting.[22] The topology was monitored by calculating the Alexander polynomial, $\Delta(x)$ for $x = -1$, along the trajectory (see ref 22 for details). If the values of δ_s and δ_r were not small enough, we observed rather fast unknotting of the chain (Figure 1). We found that for $d = b$ and $\delta_r = \delta_s = 0.07b$ the knot type was retained along very long BD trajectories, and we used these values for our nonphan-

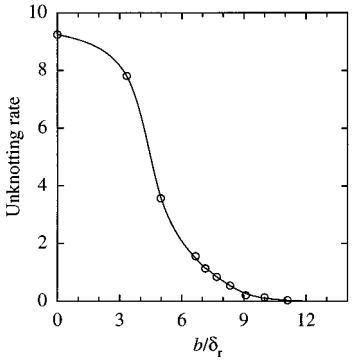

Figure 1. Test of the impenetrability of the model chain. We started the simulation of circular chain from the knotted conformation and monitored the topology. The unknotting rate, as a reciprocal of the mean unknotting time expressed in the units of b^2/D_0, is plotted vs the stretching and repulsion rigidities, δ_s and δ_r, which were equal to each other for all points but one. The data point $b/\delta_r = 0$ corresponds to the model chain without excluded volume with $\delta_s = 0.07b$. No unknottings occurred when $\delta_r = \delta_s = 0.07b$; thus, such rigid chain could be considered as nonphantom.

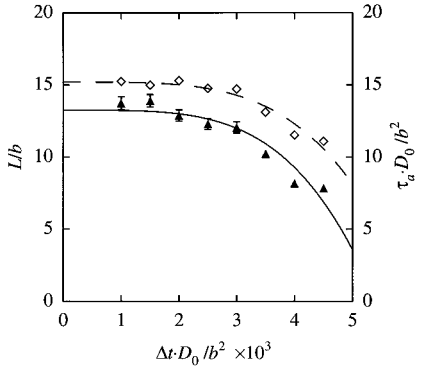

Figure 2. Choice of the time step Δt for the Brownian dynamics simulations. Varying the time step we measured the mean end-to-end distance (◇, left axis) and cyclization time (▲, right axis) of the freely jointed chains without excluded volume, $\delta_s = 0.07b$. The time step has to be chosen so that the simulation does not disturb the dynamic and static properties of the chain. It follows from the data that the time step cannot be set larger than $0.003b^2/D_0$ for this model.

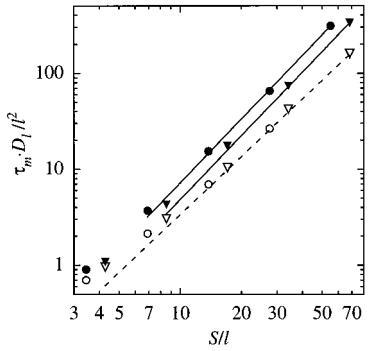

Figure 3. Dependence of the end-to-end distance relaxation time on the chain length. The data for freely jointed chains with $\delta_r = \delta_s = 0.07b$ (circles) and $\delta_r = \delta_s = 0.3b$ (triangles) are presented. For the both phantom (▼) and nonphantom (●) chains with excluded volume the slopes of the lines are equal to 2.2. The data for the chains without excluded volume (hollow symbols) are in very good agreement with the eq 6, as shown by the dashed line. The statistical error is less than the symbol size.

tom models. The chosen value of δ_s corresponds to 7% thermal fluctuations of bond lengths.

To distinguish between the effects of excluded volume itself and impenetrability, each of which can possibly affect the polymer kinetics, we investigated less rigid chains with $\delta_r = \delta_s = 0.3b$. The rate of unknotting for such chains was close to the rate for the chains with no excluded volume (see Figure 1). This allowed us to assume that these values of δ_s and δ_r almost eliminate the hindrances for bond passages through each other, leaving for consideration only the excluded volume effects.

For the hindered random walk models a value of 0.8165 was chosen for the bending rigidity parameter, δ_b.

2. Time Step. The BD algorithm requires a sufficiently large time step to neglect the bead inertia, $\Delta t \gg mD_0/kT$, where m is the bead mass.[15] The time step should be also sufficiently small to exclude large changes of the forces, $D_0\Delta t \ll \delta^2$. In the last equation δ is the fluctuation of a bead position around the equilibrium value for the most rigid potential. In our case, δ corresponded to the stretching rigidity parameter, δ_s. The chosen time step was equal to $0.003b^2/D_0$ for $\delta_r = \delta_s = 0.07b$ and $0.02b^2/D_0$ for $\delta_r = \delta_s = 0.3b$. We checked that the values of the mean end-to-end distance and autocorrelation function obtained from BD simulation with these values of Δt were in very good agreement with the corresponding values from Monte Carlo simulations and from BD simulations with smaller Δt (Figure 2).

3. Contour Length and Reaction Radius. Usually chains of up to 81 beads were studied. This corresponded to about 55 statistical segments for a rigid freely jointed chain ($\delta_r = \delta_s = 0.07b$), 70 segments for a soft freely jointed chain ($\delta_r = \delta_s = 0.3b$), and 23 segments for the hindered random walk chain. The reaction radius was varied in the range from $0.3l$ to $1.3l$. The value of statistical length, l, was estimated by the simulations for the chains without excluded volume from the equation for the end-to-end distance.

The computation time per one BD step grows linearly with chain length for the ideal chains and quadratically for the chains with excluded volume. The most time-consuming runs for the longest hindered random walk chains with excluded volume took about 20 days on an Indigo2Impact SGI workstation.

III. Results and Discussion

A. Dependence of the End-to-End Distance Relaxation Time on the Chain Length. First we studied the relaxation of the end-to-end distance and determined the end-to-end distance relaxation time, τ_m, of the model chains (Figure 3). For ideal chains of more than 15 statistical segments the values of τ_m were in excellent quantitative agreement with the theoretical result for the Rouse chain

$$\tau_m = \frac{1}{3\pi^2}\frac{\langle L^2\rangle}{D} \qquad (6)$$

where D is the diffusion coefficient of the whole polymer molecule, and $\langle L^2\rangle$ is the mean square end-to-end distance.[1] The line corresponding to (6) is also shown in Figure 3. The shorter chains have higher values of τ_m than predicted by the Rouse model.

The values of τ_m of the long chains with excluded volume were proportional to $S^{2.2\pm0.1}$, where S is the chain length (Figure 3). This is in agreement with the theoretical estimate for a Rouse chain with excluded

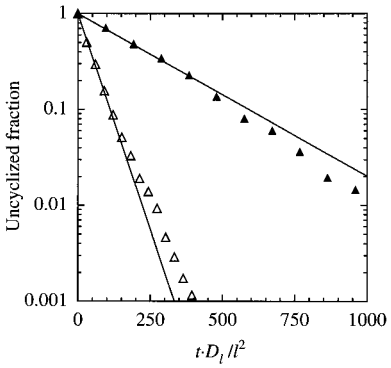

Figure 4. Kinetics of chain cyclization. The data for the freely jointed chains, $S = 22l$, $\delta_r = \delta_s = 0.07b$, were fitted by a single exponent. The reciprocals of the cyclization rates, slopes of the straight lines, are equal to $(256 \pm 4)l^2/D_l$ and $(48.2 \pm 0.7)l^2/D_l$ for the chain with (▲) and without (△) excluded volume respectively, where D_l is the diffusion coefficient of the statistical length ($D_l = D_0 b/l$). These values are in good agreement with the corresponding mean cyclization times, $(254 \pm 11)l^2/D_l$ and $(49 \pm 2)l^2/D_l$.

volume.[4] We obtained the same exponent for both the nonphantom and phantom chains which differed by the stretching potential and the potential specifying excluded volume (see section II for details). Thus, within the accuracy of our simulations, the impenetrability itself did not change the exponent of the dependence. The value of the exponent is determined only by the presence of excluded volume in the model.

The exponent 2.2 can be obtained assuming that τ_m is proportional to $\langle L^2 \rangle / D$ as it is for the Rouse chain (see (6)) if we take into account that $\langle L^2 \rangle \propto S^{1.2}$ for the chains with excluded volume.[23] We found, however, that the coefficient of the proportionality was different from $1/3\pi^2$ for our model chains with excluded volume. To evaluate the actual coefficient, which can be written as $\xi/3\pi^2$, the values of $\langle L^2 \rangle$ were calculated by Monte Carlo simulations. For the nonphantom freely jointed and hindered random walk chains the values of ξ were equal to 1.4 ± 0.1 and 1.6 ± 0.1 respectively. It is notably larger than the value of ξ for the phantom freely jointed chains, which was equal to 1.15 ± 0.05. Thus, we see that impenetrability of the chains causes an increase of the end-to-end distance relaxation time by a factor close to 1.5.

B. Dependence of the Cyclization Time on Chain Length. Wilemski and Fixman found that the time decay of the fraction of uncyclized molecules due to irreversible cyclization is described by a sum of exponential terms, with the first one strongly dominating the others.[7] Under certain conditions it accounts for 99% of the total sum. We tested this theoretical conclusion by the simulations (Figure 4). It is clear from the figure that the decay of the uncyclized fraction is very well described by a single exponential decay for the early 90% of cyclizations at least. Thus, the description of the cyclization reaction by a single-exponential decay is a very accurate approximation, and we can talk about the first-order cyclization rate constant. This simplifies the following comparison of our results obtained for the cyclization time with the known analytical equations, most of which were obtained for the cyclization rates. We have to note, however, that small deviations from a single exponential decay seen in Figure 4 for the long time are statistically meaningful.

The dependence of the cyclization time, τ_a, as a function of S for the freely jointed and hindered random walk models is shown in Figure 5. For S greater than 15 statistical lengths, the dependence can be approximated as $\tau_a \propto S^{\beta}$.

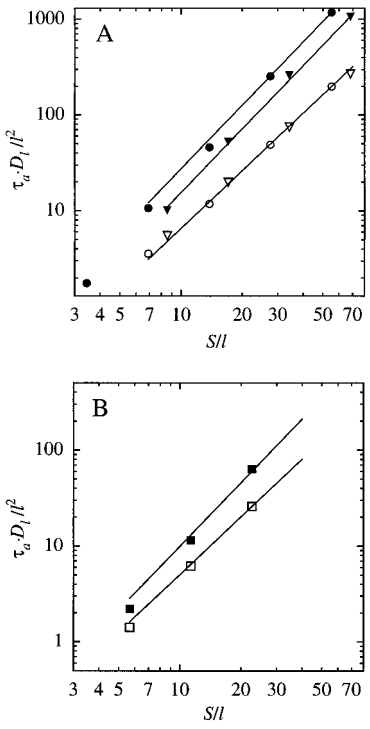

Figure 5. Dependence of cyclization time on chain length. (A) The data for freely jointed chains with $\delta_r = \delta_s = 0.07b$ (circles) and $\delta_r = \delta_s = 0.3b$ (triangles) are presented. For both phantom (▼) and nonphantom (●) chains with excluded volume, the slopes of the lines are equal to 2.2. For chain without excluded volume (hollow symbols) the slope is equal to 2.0. (B) The data for the hindered random walk models. For nonphantom chains with excluded volume (■), the slope of the line is equal to 2.2; for chains without excluded volume (□), the slope is equal to 2.0. The statistical error was less than the symbol size. The reaction radius was equal to $0.7l$.

For the phantom chains without excluded volume the exponent β was equal to 2.0 ± 0.1, while it was equal to 2.2 ± 0.1 for both the nonphantom and phantom chains with excluded volume. Thus, the exponent was affected only by excluded volume. The quantitatively similar difference between the exponents for chains with and without excluded volume was observed in the experimental studies of polysterene cyclization in good and in a Θ-solvent.[14]

For ideal chains the proportionality of τ_a to the square of contour length, S, is in a good agreement with the analytical results.[8,11] The Rouse model without hydrodynamic interactions and excluded volume gives an unexpectedly simple expression for τ_a

$$\tau_a = \frac{\pi^3}{16}\tau_m \propto S^2 \tag{7}$$

where τ_m is the end-to-end distance relaxation time. However, the independence of τ_a on the reaction radius is inconsistent with our data (see below).

Our results for the dependence of τ_a on S for chains with excluded volume, $\tau_a \propto S^{2.2\pm0.1}$, agree with the estimation obtained by Friedman and O'Shaughnessy[11,13] for the free-draining Rouse chain with excluded volume:

$$\tau_a = \frac{\pi^3}{8}\tau_m \propto S^{2.2} \tag{8}$$

Table 1. Dependence of the Cyclization Time on the Reaction Radius

S/l	R/l	$\tau_a D_l/l^2$	model
14	0.3	80 ± 2	freely jointed
14	0.7	37.7 ± 1.8	
14	1.3	19 ± 2	
28	0.3	253 ± 13	
28	0.7	156 ± 5	
55	0.7	653 ± 32	
55	1.3	266 ± 43	
6	0.3	53.5 ± 2.6	hindered random walk
6	0.7	14.7 ± 0.9	
12	0.3	187 ± 11	
12	0.7	61.6 ± 3.6	
23	0.3	593 ± 37	
23	0.44	409 ± 16	
23	0.7	270 ± 12	

We observed deviations from the discussed asymptotic dependencies for the chains shorter than 15 statistical segments. Namely, for the chains without excluded volume the power was less than 2 in agreement with the prediction for short ideal chains, $\tau_a \propto S^{1.5}$.[13] The shorter chains with excluded volume show a stronger dependence on S with an exponent greater than 2.2 because of the large excluded volume of the statistical segment in our models.

C. The Dependence of Cyclization Time on Reaction Radius. We studied the dependence of τ_a on the reaction radius, R, for $0.3l \le R \le 1.3l$. Simulated values of τ_a for different chain lengths are shown in Table 1. Despite the rather large statistical error of the data, they are consistent with the reciprocal proportionality of τ_a to R both for the freely jointed and hindered random walk chains.

This reciprocal proportionality is inconsistent with (7) and (8), for which there is no dependence on the reaction radius at all. These expressions were derived for the Rouse chain model and should be valid for more realistic chains only when $l \ll R \ll L$.[8] This is far from the conditions of our simulations, $l \approx R \ll L$; therefore, one could expect inconsistencies. For $R \ll l$, Doi suggested that τ_a is proportional to l/R.[8]

There was an attempt to describe the cyclization behavior of a polymer chain with the harmonic-spring model, in which the chain end-to-end vector was specified only as a harmonic oscillator.[8,9] This very naive model predicts the dependence of τ_a on R in agreement with the simulation results

$$\tau_a = \frac{1}{\sqrt{2}} \frac{L}{R} \tau_m \propto S^{2.5} \tag{9}$$

where L is the root mean square end-to-end distance. It does not give the correct dependence on S, however.

The much more realistic wormlike chain model was considered by Berg.[10] He found the following expression for the cyclization time:

$$\tau_a \approx 12 \frac{l^2}{D_l} \left(\frac{S}{l}\right)^{3/2} \left(\frac{l}{R}\right)^{1/3} \tag{10}$$

Here, D_l is the diffusion coefficient of a statistical segment. Although the range of R where eq 10 was supposed to be valid corresponds well to our conditions, the equation does not agree with the simulation results. The dependence of τ_a on S in (10) also contradicts the simulation results.

The reciprocal proportionality between cyclization time and reaction radius was also detected in other recent computer simulations[18,19] and in the theoretical analysis combined with numerical integration.[12] Although it is very difficult to vary R in experiments with actual polymers, there are data showing a dependence of τ_a on R.[14]

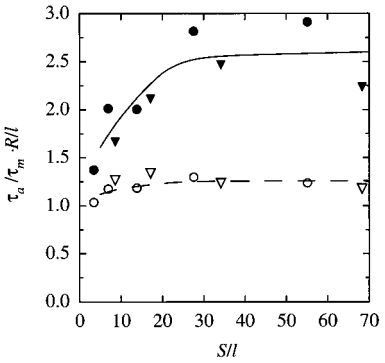

Figure 6. Ratio of the cyclization time to the end-to-end distance relaxation time. The data for freely jointed chains with $\delta_r = \delta_s = 0.07b$ (circles) and $\delta_r = \delta_s = 0.3b$ (triangles) are presented. The solid line approximates the data for both phantom (▼) and nonphantom (●) chains with excluded volume; the dashed line corresponds to the phantom chains without excluded volume (hollow symbols). The statistical error is about 15%. R/l was equal to 0.7.

D. Comparison of the Cyclization and Relaxation Times. Equations 7 and 8 predict certain constant values of τ_a/τ_m for Rouse chains with and without excluded volume. We were not able to verify this theoretical prediction, since we examined the range of R where τ_a depended on R. Our numerical results did allow us, however, to test the theoretical predictions about the relative change in τ_a/τ_m caused by the excluded volume effect.

Figure 6 shows that for the chains without excluded volume the ratio τ_a/τ_m was largely independent of S for our models and was equal to 1.3 ± 0.2. For the chains with excluded volume the ratio initially grows with increasing chain length and then appears to reach a constant value (Figure 6). We did not find a reliable difference between the values of τ_a/τ_m for the phantom and nonphantom chains. Thus, our result show that τ_a/τ_m does not depend on impenetrability effects. It follows from the data that for the chains longer than 20 statistical segments τ_a/τ_m was equal to 2.6 ± 0.3 although we are not sure whether this is the upper limit of the value. This 2-fold difference of τ_a/τ_m between the chains with and without excluded volume is in a good agreement with (7) and (8).

IV. Conclusions

In this work we tried to estimate the importance of topological hindrances emerging in polymer motion and their influence on the dynamic characteristics of polymers, such as τ_m and τ_a. Brownian dynamics simulations allowed us to consider more realistic models of a polymer chain than usually used in analytical treatment of the problem. At the same time, we did not take into account the hydrodynamic interaction between chain segments to obtain data for longer chains. Although the hydrodynamic interaction affects the relaxation properties of a polymer chain, we believe that it should not change our estimation of impenetrability effects. An accurate test of this assumption can be a subject of future work.

We found that the impenetrability of the chains appeared to have small effect on the magnitude of τ_m,

exceeding the value for the phantom chains by a factor of 1.5. The cyclization time, which scales as τ_m, did not undergo any additional increase due to chain impenetrability alone. On the other hand, the excluded volume effect changed the power of the dependence of τ_m on the chain contour length, in accordance with theoretical conclusions. In addition, the presence of the excluded volume caused the 2-fold growth of the scaling factor between τ_a and τ_m for sufficiently long chains. This scaling factor and, consequently, τ_a appeared to be reciprocally proportional to the reaction radius.

We can generalize our results in the form of empirical equations for τ_a and τ_m

$$\tau_m = \frac{\xi}{3\pi^2}\frac{\langle L^2\rangle}{D} \tag{11}$$

where the coefficient ξ is equal to 1.0 ± 0.1 and 1.5 ± 0.1 for phantom and nonphantom chains correspondingly, and

$$\tau_a = \zeta\frac{l}{R}\tau_m \tag{12}$$

where the coefficient ζ is equal to 1.3 ± 0.2 and 2.6 ± 0.3 for chains without and with excluded volume correspondingly. According to the simulation results, the equations are valid for chains longer than 20 statistical segments and for a reaction radius of about one statistical segment.

Acknowledgment. The authors thank J. Marko for helpful discussions. This work was supported in part by the National Institutes of Health (grant No. GM54215 to AV).

References and Notes

(1) Rouse, P. E., Jr. *J. Chem. Phys.* **1953**, *21*, 1272.
(2) Zimm, B. H. *J. Chem. Phys.* **1956**, *24*, 269.
(3) Harris, R. A.; Hearst, J. E. *J. Chem. Phys.* **1966**, *44*, 2595.
(4) Oono, Y.; Freed, K. F. *J. Chem. Phys.* **1981**, *75*, 1009.
(5) Wilemski, G.; Fixman, M. *J. Chem. Phys.* **1973**, *58*, 4009.
(6) Wilemski, G.; Fixman, M. *J. Chem. Phys.* **1974**, *60*, 866.
(7) Wilemski, G.; Fixman, M. *J. Chem. Phys.* **1974**, *60*, 878.
(8) Doi, M. *Chem. Phys.* **1975**, *9*, 455.
(9) Battezzati, M.; Perico, A. *J. Chem. Phys.* **1981**, *74*, 4527.
(10) Berg, O. G. *Biopolymers* **1984**, *23*, 1869.
(11) Friedman, B.; O'Shaughnessy, B. *Phys. Rev. A* **1989**, *40*, 5950.
(12) Perico, A.; Beggiato, M. *Macromolecules* **1990**, *23*, 797.
(13) Friedman, B.; O'Shaughnessy, B. *Macromolecules* **1993**, *26*, 4888.
(14) Winnik, W. A. In *Cyclic Polymers*; Semlyen, J. A., Ed.; Elsvier: New York, 1986.
(15) Ermak, D. L.; McCammon, J. A. *J. Chem. Phys.* **1978**, *69*, 1352.
(16) Iniesta, A.; Garcia de la Torre, J. *J. Chem. Phys.* **1990**, *92*, 2015.
(17) Cuniberti, C.; Perico, A. *Prog. Polym. Sci.* **1984**, *10*, 271.
(18) Garcia Fernandez, J. L.; Rey, A.; Freire, J. J.; de Pierola, I. F. *Macromolecules* **1990**, *23*, 2057.
(19) Rey, A.; Freire, J. J. *Macromolecules* **1991**, *24*, 4673.
(20) Metropolis, N.; Rosenbluth, A. W.; Rosenbluth, M. N.; Teller, A. H.; Teller, E. *J. Chem. Phys.* **1953**, *21*, 1087.
(21) Allison, S. A. *Macromolecules* **1986**, *19*, 118.
(22) Vologodskii, A. V.; Lukashin, A. V.; Frank-Kamenetskii, M. D.; Anshelevich, V. V. *Sov. Phys. JETP* **1974**, *39*, 1059.
(23) Flory, P. J. *Statistical mechanics of chain molecules*; Wiley: New York, 1969.

MA970391A